Controlled Spacing of Few-Layer Graphene Sheets Using Molecular Spacers: Capacitance that Scales with Sheet Number

Anna K. Farquhar, Paula A. Brooksby*, Alison J. Downard*

MacDiarmid Institute of Advanced Materials and Nanotechnology, School of Physical and Chemical Sciences, University of Canterbury, Private Bag 4800, Christchurch 8140, New Zealand

Email: Paula.brooksby@canterbury.ac.nz; Alison.downard@canterbury.ac.nz

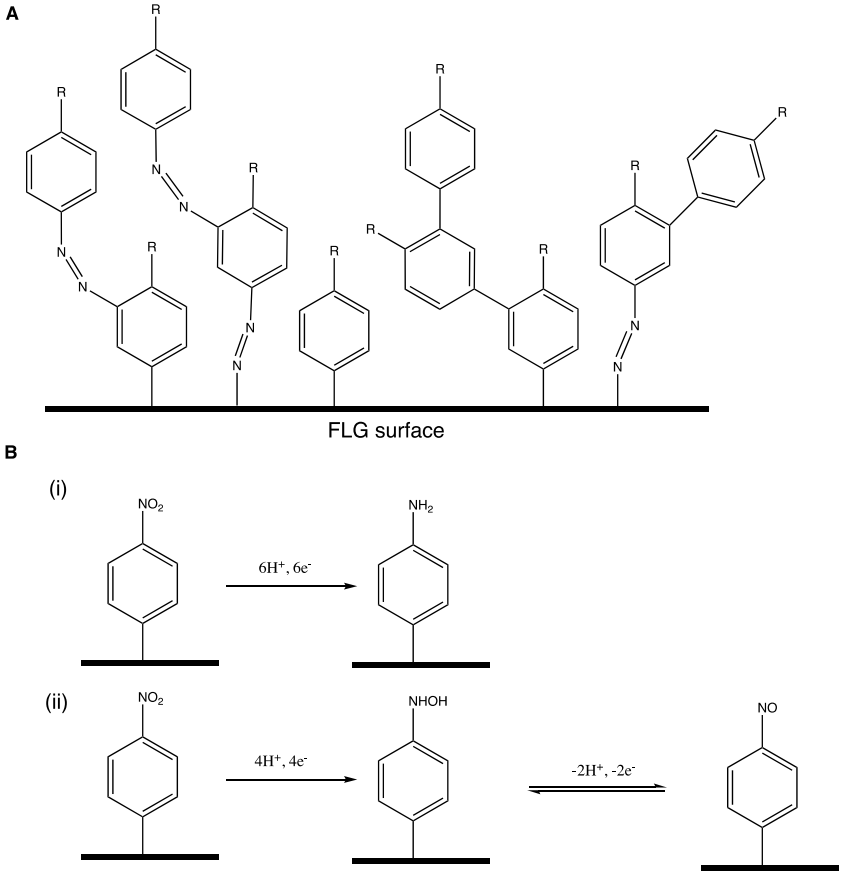

Scheme S1: (A) Generalized structure for a multilayer film grafted from aryldiazonium salts;[1] (B) In acidic conditions, electrochemical reduction of a nitrophenyl (NP) layer converts the majority of groups to aminophenyl (AP) groups via a 6 electron, 6 proton step (i) with some NP groups undergoing a 4 electron, 4 proton reduction to hydroxylaminophenyl groups (ii). Hydroxylaminophenyl groups can be reversibly oxidized with the loss of 2 electrons and 2 protons to nitrosophenyl groups (ii). Measuring the charge associated with the reduction of NP groups and oxidation of hydroxylaminophenyl groups allows the surface concentration of NP groups to be determined.

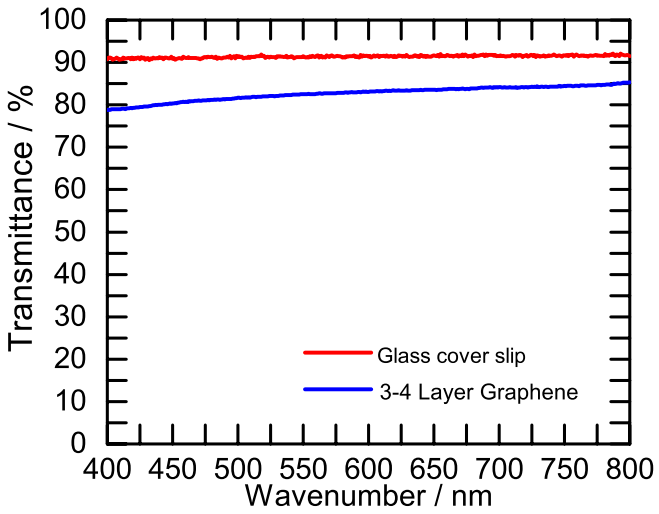

Figure S1: Visible spectra of a glass microscope coverslip (red) and FLG on the coverslip (blue). Geim et al. have shown that the transparency between 600 and 800 nm changes by 2.3% for each graphene layer.[2] Hence the FLG used in the present work has 3-4 graphene layers.

Characterization of Modified FLG by FTIR and Atomic Force Microscopy (AFM)

FTIR spectra were collected using a Bruker Vertex 70 spectrometer operating OPUS software. Spectra were recorded in either transmission or attenuated total reflection (ATR) mode. Spectra were collected using 32 scans at 4 cm^{-1} resolution from 600 to 4000 cm^{-1} with a liquid nitrogen cooled MCT detector. For transmission mode spectra, the free-floating graphene (modified or unmodified), was collected onto a KBr disk from a water bath, dried in air for 30 minutes and at 60 ^{o}C for 30 minutes. The samples were then rinsed with methanol and dried for a further 15 minutes. A background spectrum of a bare KBr disk was collected prior to recording the FLG spectra.

AFM (Digital Instruments Dimensions 3100) topographical measurements were done in noncontact tapping mode with a silicon cantilever (Tap 300Al-G) operating at resonant frequencies of approximately 280 kHz. Images were collected at a scan rate of 0.5 Hz with 512 samples per line. For AFM imaging, free-floating graphene (modified or unmodified) was collected onto a freshly cleaved HOPG substrate. As the FLG_{CP} sample was modified after removal of the FLG from the copper, the CP groups were sandwiched between the FLG and the HOPG substrate after collection. In order to view the modified side of the FLG_{CP}, the FLG_{CP} was first collected onto a KBr disk, which was subsequently submerged upside down in a water bath, to release the FLG_{CP} with the CP groups face-up, so the FLG_{CP} could be collected onto the HOPG with the groups in an exposed orientation.

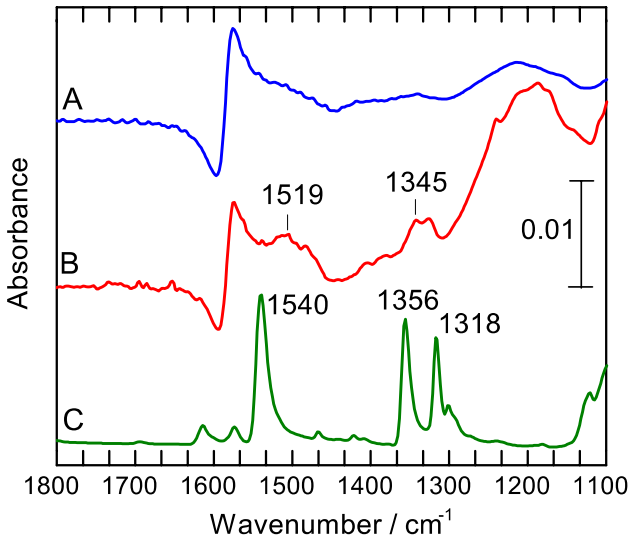

Figure S2: IR spectra of (A) FLG; (B) FLG_{NP}; and (C) NBD precursor. Spectra A and B collected in transmission mode. NBD precursor spectrum collected in ATR mode and scaled 0.08×. Spectra offset for clarity. Peak assignments:[3-7] 1519/1540 cm^{-1} NO_2 asymmetric stretch, 1356/1345 cm^{-1} NO_2 symmetric stretch.

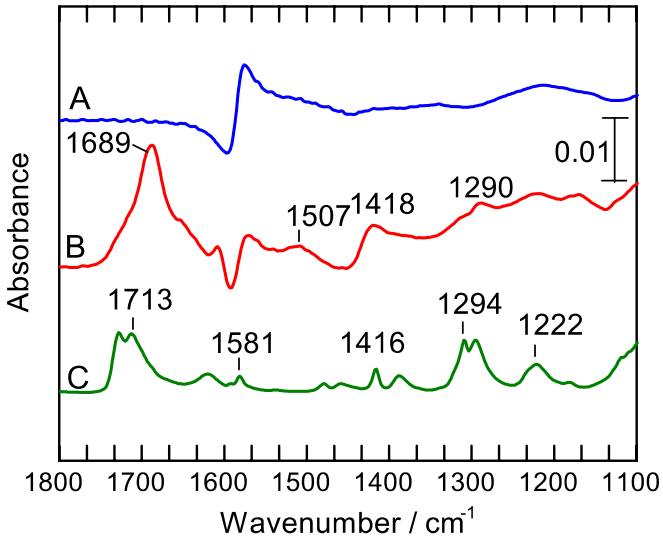

Figure S3: IR spectra of (A) FLG; (B) FLG_{CP}; and (C) CBD precursor. Spectra A and B obtained in transmission mode. CBD precursor spectrum collected in ATR mode and scaled 0.05×. Spectra offset for clarity. Peak assignments:[8,9] 1713/1689 cm^{-1} C=O stretch and CCO bend, 1294/1290 cm^{-1} C-O stretch and COH bend.

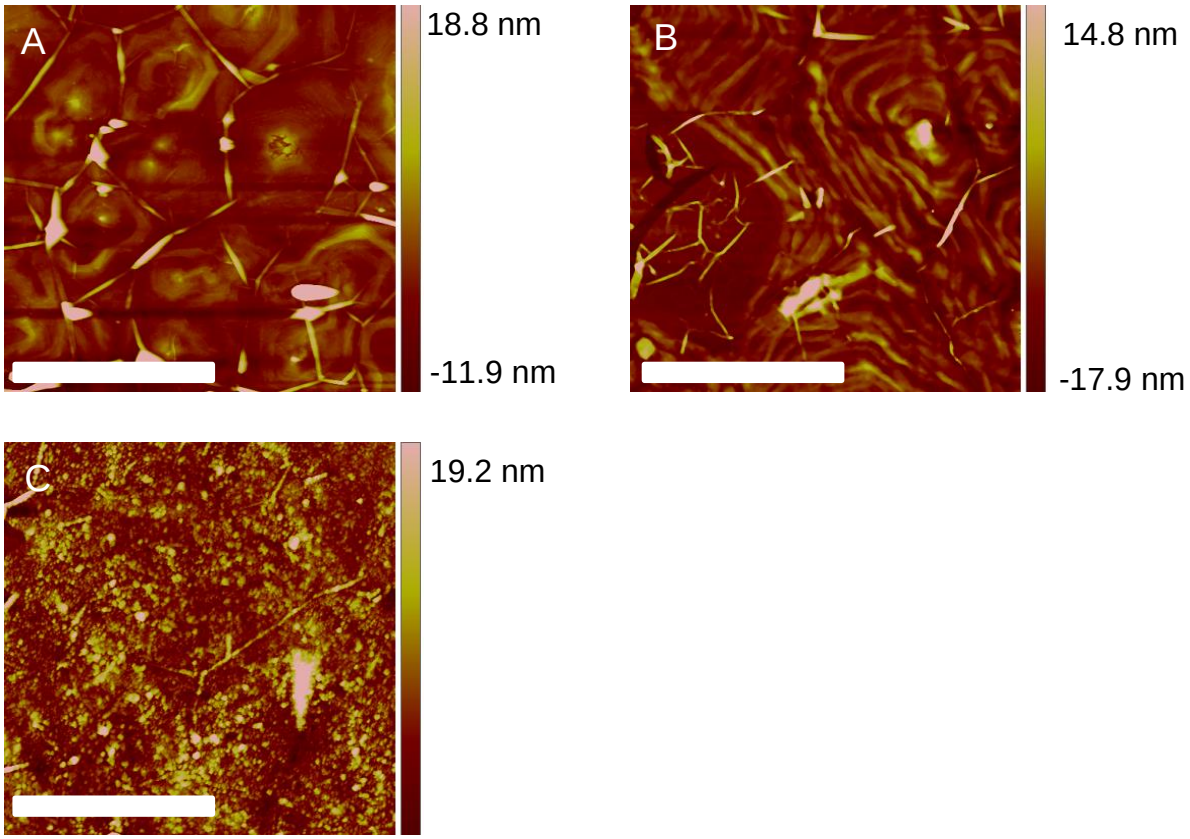

Figure S4: AFM images of FLG on HOPG: (A) FLG; (B) FLG_{CP} with CP groups sandwiched between FLG and HOPG; and (C) FLG_{CP} with CP groups exposed, after flipping FLG_{CP} using KBr disk. Scale bar = 2.5 μm. The absence of any new features in (B) confirms the modification takes place on one side of the FLG sheet only.

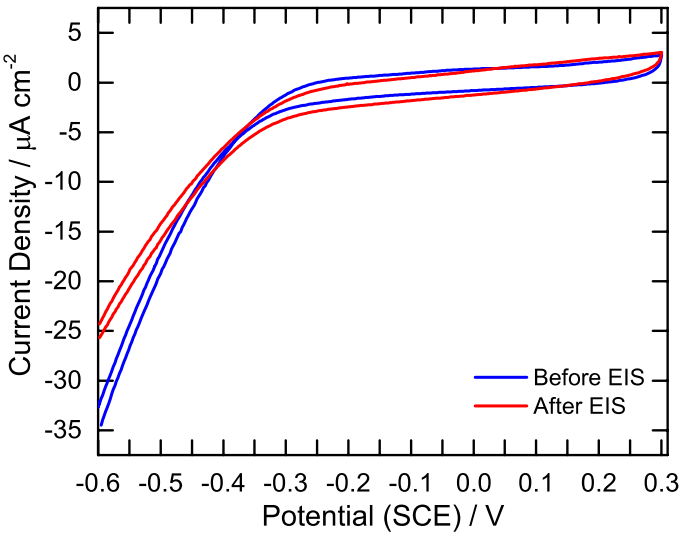

Figure S5: CV of FLG before and after EIS in 1 M $HClO_4$. Scan rate = 200 mV s^{-1}.

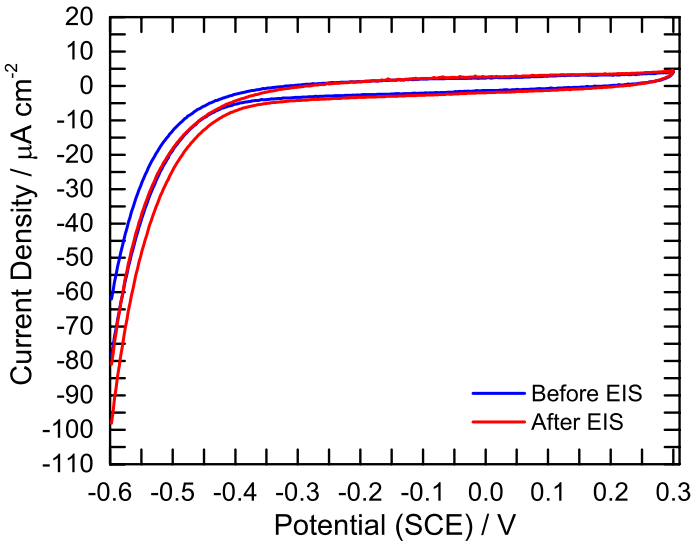

Figure S6: CV of FLG_{AP} before and after EIS in 1 M $HClO_4$. Scan rate = 200 mV s^{-1}.

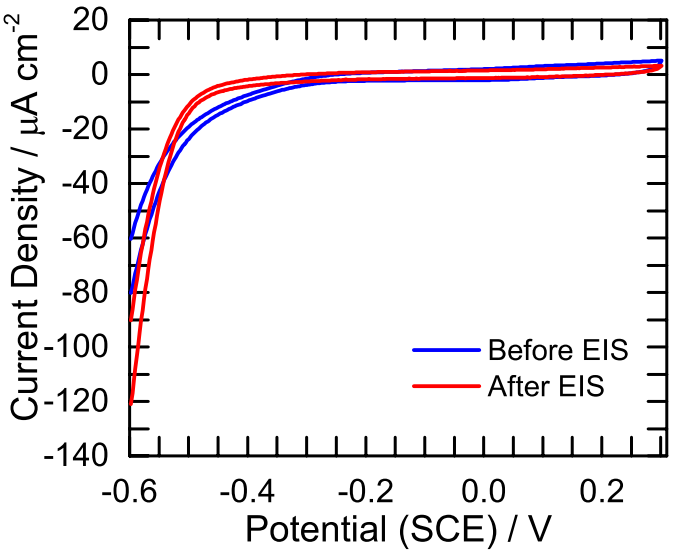

Figure S7: CV of FLG_{CP} before and after EIS in 1 M $HClO_4$. Scan rate = 200 mV s^{-1}.

Nyquist plots of Single FLG sheets and 3-sheet stacks

Figures S8 and S9 show Nyquist plots obtained at 100 mV in 1 M $HClO_4$. For all plots, there is no semicircle in the high frequency region, consistent with negligible interfacial charge transfer resistance as expected for purely electrical double capacitive behavior.[10-13] In all five systems, a short line with an angle close to 45^o exists in the mid-frequency region, which is characteristic of a Warburg impedance. This is very short for all systems, indicating fast ion diffusion to the FLG surfaces.[10,12,14-16] At low frequencies, an almost vertical tail for each system demonstrates excellent electrical double layer capacitive behavior.[10,16,17]

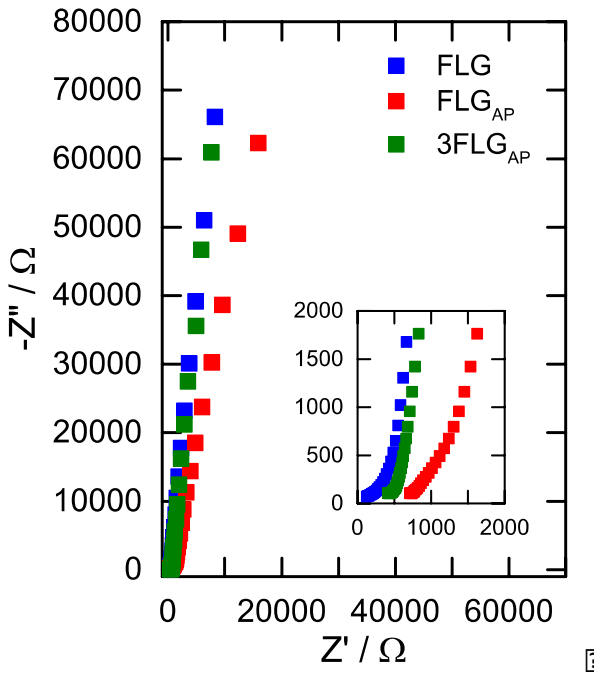

Figure S8: Nyquist plots of FLG, FLG_{AP}, and $3FLG_{AP}$, recorded at 100 mV, in 1 M $HClO_4$. The plots are consistent with significantly higher solution resistance at the FLG_{AP} electrode than at the FLG and $3FLG_{AP}$ electrodes; the origin of this phenomenon is unclear.

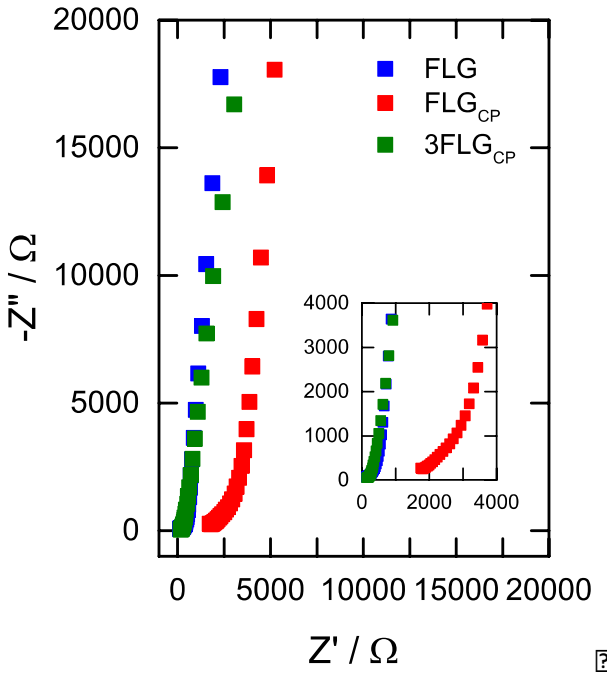

Figure S9: Nyquist plots of FLG, FLG_{CP}, and $3FLG_{CP}$, recorded at 100 mV, in 1 M $HClO_4$. The plots are consistent with significantly higher solution resistance at the FLG_{CP} electrode than at the FLG and $3FLG_{CP}$ electrodes; the origin of this phenomenon is unclear.

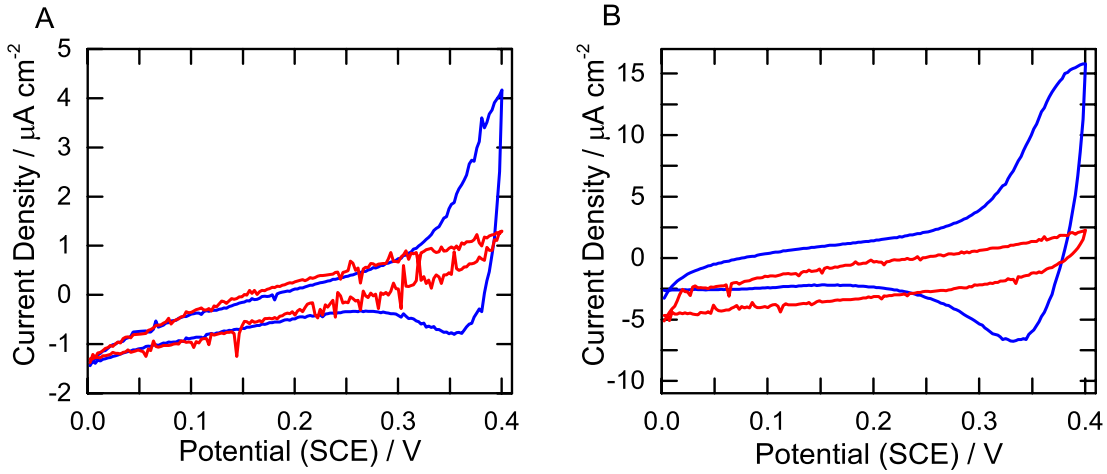

Figure S10: CVs in 1 M $HClO_4$ before (blue) and after (red) 20,000 CD cycles at 10 μA cm^{-2}: (A) FLG_{AP} and (B) $3FLG_{AP}$. Scan rate = 50 mV s^{-1}.

References

(1) Doppelt, P.; Hallais, G.; Pinson, J.; Podvorica, F.; Verneyre, S. Surface Modification of Conducting Substrates. Existence of Azo Bonds in the Structure of Organic Layers Obtained from Diazonium Salts. *Chem. Mater.* **2007**, *19*, 4570-4575.

(2) Nair, R. R.; Blake, P.; Grigorenko, A. N.; Novoselov, K. S.; Booth, T. J.; Stauber, T.; Peres, N. M. R.; Geim, A. K. Fine Structure Constant Defines Visual Transparency of Graphene. *Science* **2008**, *320*, 1308-1308.

(3) Anariba, F.; Viswanathan, U.; Bocian, D. F.; McCreery, R. L. Determination of the Structure and Orientation of Organic Molecules Tethered to Flat Graphitic Carbon by ATR-FT-IR and Raman Spectroscopy. *Anal. Chem.* **2006**, *78*, 3104-3112.

(4) Cullen, R. J.; Jayasundara, D. R.; Soldi, L.; Cheng, J. J.; Dufaure, G.; Colavita, P. E. Spontaneous Grafting of Nitrophenyl Groups on Amorphous Carbon Thin Films: A Structure–Reactivity Investigation. *Chem. Mater.* **2012**, *24*, 1031-1040.

(5) Murphy, D. M.; Cullen, R. J.; Jayasundara, D. R.; Scanlan, E. M.; Colavita, P. E. Study of the Spontaneous Attachment of Polycyclic Aryldiazonium Salts onto Amorphous Carbon Substrates. *RSC Advances* **2012**, *2*, 6527-6534.

(6) Pandurangappa, M.; Ramakrishnappa, T.; Compton, R. G. Functionalization of Glassy Carbon Spheres by Ball Milling of Aryl Diazonium Salts. *Carbon* **2009**, *47*, 2186-2193.

(7) Richner, G.; van Bokhoven, J. A.; Neuhold, Y.-M.; Makosch, M.; Hungerbuhler, K. In Situ Infrared Monitoring of the Solid/Liquid Catalyst Interface During the Three-Phase Hydrogenation of Nitrobenzene over Nanosized Au on TiO_2. *PCCP* **2011**, *13*, 12463-12471.

(8) Chehimi, M. M.; Lamouri, A.; Picot, M.; Pinson, J. Surface Modification of Polymers by Reduction of Diazonium Salts: Polymethylmethacrylate as an Example. *J. Mater. Chem. C* **2014**, *2*, 356-363.

(9) Krishnakumar, V.; Mathammal, R. Density Functional and Experimental Studies on the FT-IR and FT-Raman Spectra and Structure of Benzoic Acid and 3,5-Dichloro Salicylic Acid. *J. Raman Spectrosc.* **2009**, *40*, 264-271.

(10) Zhang, D.; Zhang, X.; Chen, Y.; Yu, P.; Wang, C.; Ma, Y. Enhanced Capacitance and Rate Capability of Graphene/Polypyrrole Composite as Electrode Material for Supercapacitors. *J. Power Sources* **2011**, *196*, 5990-5996.

(11) Luo, J.; Ma, Q.; Gu, H.; Zheng, Y.; Liu, X. Three-Dimensional Graphene-Polyaniline Hybrid Hollow Spheres by Layer-by-Layer Assembly for Application in Supercapacitor. *Electrochim. Acta* **2015**, *173*, 184-192.

(12) Wu, M.; Li, Y.; Yao, B.; Chen, J.; Li, C.; Shi, G. A High-Performance Current Collector-Free Flexible in-Plane Micro-Supercapacitor Based on a Highly Conductive Reduced Graphene Oxide Film. *J. Mater. Chem. A* **2016**, *4*, 16213-16218.

(13) Bi, H.; Lin, T.; Xu, F.; Tang, Y.; Liu, Z.; Huang, F. New Graphene Form of Nanoporous Monolith for Excellent Energy Storage. *Nano Lett.* **2016**, *16*, 349-354.

(14) Shao, Y.; El-Kady, M. F.; Lin, C.-W.; Zhu, G.; Marsh, K. L.; Hwang, J. Y.; Zhang, Q.; Li, Y.; Wang, H.; Kaner, R. B. 3d Freeze-Casting of Cellular Graphene Films for Ultrahigh-Power-Density Supercapacitors. *Adv. Mater.* **2016**, *28*, 6719-6726.

(15) Robat Sarpoushi, M.; Reza Borhani, M.; Nasibi, M.; Eghdami, B.; Kazerooni, H. Graphene Nanosheets as Electrode Materials for Supercapacitors in Alkaline and Salt Electrolytes. *Mater. Sci. Semicond. Process.* **2015**, *31*, 195-199.

(16) Walsh, E. D.; Han, X.; Lacey, S. D.; Kim, J.-W.; Connell, J. W.; Hu, L.; Lin, Y. Dry-Processed, Binder-Free Holey Graphene Electrodes for Supercapacitors with Ultrahigh Areal Loadings. *ACS Appl. Mater. Interfaces* **2016**, *8*, 29478-29485.

(17) Taberna, P.; Simon, P.; Fauvarque, J.-F. Electrochemical Characteristics and Impedance Spectroscopy Studies of Carbon-Carbon Supercapacitors. *J. Electrochem. Soc.* **2003**, *150*, A292-A300.